Spectroscopic Investigation of Yb-Doped Silica Glass for Solid-State Optical Refrigeration

Esmaeil Mobini,[1,2] Mostafa Peysokhan,[1,2] Behnam Abaie,[1,2] Markus P. Hehlen,[1,3] and Arash Mafi[1,2,*]

[1] *Department of Physics & Astronomy, University of New Mexico, Albuquerque, New Mexico 87131, USA*
[2] *Center for High Technology Materials, University of New Mexico, Albuquerque, New Mexico 87106, USA*
[3] *Space & Remote Sensing (ISR-2), Los Alamos National Laboratory, Los Alamos, New Mexico 87545, USA*

(Received 24 October 2018; revised manuscript received 22 December 2018; published 31 January 2019)

We argue that a high-purity Yb-doped silica glass can potentially be cooled via anti-Stokes-fluorescence optical refrigeration. In order to achieve net solid-state optical refrigeration, it is necessary for the cooling efficiency to be positive. This requires the pump wavelength to be greater than the mean fluorescence wavelength and the internal quantum efficiency as well as the absorption efficiency to be near unity. Our conclusion is reached by showing, using reasonable assumptions for the host-material properties, that the nonradiative decay rate of Yb ions can be made substantially smaller than the radiative decay rate. Therefore, an internal quantum efficiency of near unity can be obtained. Moreover, the background absorption coefficient in high-quality silica glass lies in an acceptable range to guarantee a near-unity absorption efficiency at room temperature. Using spectral measurements of the fluorescence from a Yb-doped silica optical fiber at a range of temperatures, we estimate the minimum achievable temperature in Yb-doped silica glass for different values of the internal quantum efficiency.

DOI: 10.1103/PhysRevApplied.11.014066

I. INTRODUCTION

In solid-state optical refrigeration, anti-Stokes fluorescence removes thermal energy from the material, resulting in net cooling. Solid-state optical cooling was first proposed by Pringsheim in 1929 [1] and was put on a solid thermodynamic foundation by Landau in 1946 [2]. Solid-state optical cooling was first experimentally observed in 1995 by Epstein's group at Los Alamos National Laboratory in Yb-doped ZBLANP (ZrF_4-BaF_2-LaF_3-AlF_3-NaF-PbF_2) glass [3]. Much attention has since been devoted to solid-state optical refrigeration in various materials and geometries due to its interesting basic science properties and potential applications [4]. The quest for solid-state optical cooling in new configurations and materials is ongoing [5].

In particular, solid-state optical refrigeration of Yb-doped silica glass, which is used extensively in high-power fiber lasers, is highly desirable. New generations of high-power fiber amplifiers and lasers now operate at levels of a few kilowatts [6]. However, the significant heat load in high-power operation has hindered the efforts to further scale up the power in fiber lasers and amplifiers [6–9]. Various methods have been developed to manage the heat load in high-power fiber lasers or amplifiers; in particular, solid-state optical refrigeration via anti-Stokes fluorescence has been suggested as a viable path for heat mitigation [10–12]. So far, there is no report of solid-state optical refrigeration in Yb-doped silica; this paper is intended to highlight its possibility.

In this context, radiation-balanced lasers (RBLs) were first introduced by Bowman in 1999 [10]. In radiation balancing, the heat that originates from the quantum defect of the laser as well as parasitic absorption can be removed by anti-Stokes fluorescence under a very subtle balance condition between different parameters of a laser (or an amplifier) [10,11,13]. In other words, the anti-Stokes fluorescence removes the excess heat generated in the medium. Therefore, heat mitigation by radiation balancing via anti-Stokes fluorescence is highly desirable and will have great practical implications if it can be achieved in Yb-doped silica glass, which is the material of choice for most high-power fiber lasers and amplifiers [6,14,15].

Although the first solid-state optical refrigeration was observed in a Yb-doped ZBLAN (ZrF_4-BaF_2-LaF_3-AlF_3-NaF) glass, it soon became apparent that rare-earth-doped crystals can be cooled more efficiently because (i) the absorption lines of the Yb ions in crystals have a smaller inhomogeneous broadening and (ii) crystals can accept higher concentrations of rare-earth ions [4,5]. As such, rare-earth-doped crystals have become the material of choice for solid-state optical refrigeration [16]. Only recently has there been a renewed interest in glasses,

*mafi@unm.edu

mainly because of their potential in RBL fiber lasers and amplifiers [12].

The investigation of solid-state optical refrigeration can be done either directly or indirectly. In a direct investigation, the material is exposed to a laser in a thermally isolated setup, often in a sophisticated vacuum environment [16], and its temperature is measured directly by a thermal camera or similar methods. In an indirect method, the spectroscopic properties of materials at a range of temperatures are measured to evaluate the possibility of solid-state optical refrigeration [3,16–18]. In this paper, we use the indirect method to argue for the potential of high-quality Yb-doped silica glass for solid-state optical refrigeration and radiation balancing in lasers and amplifiers.

In order to characterize the cooling potential of Yb-doped silica glass, we use the cooling efficiency η_c, defined as [16,18]

$$\eta_c(\lambda_p, T) = \eta_q \eta_{\text{abs}}(\lambda_p, T) \frac{\lambda_p}{\lambda_f(T)} - 1. \tag{1}$$

In Eq. (1), λ_f is the mean fluorescence wavelength and λ_p is the pump wavelength. η_q is the internal quantum efficiency and η_{abs} is the absorption efficiency; they are defined as follows:

$$\eta_q = \frac{W_r}{W_{\text{tot}}}, \quad W_{\text{tot}} = W_r + W_{\text{nr}}, \tag{2}$$

$$\eta_{\text{abs}}(\lambda_p, T) = \frac{\alpha_r(\lambda_p, T)}{\alpha_r(\lambda_p, T) + \alpha_b}, \tag{3}$$

where W_r, W_{nr}, and W_{tot} are the radiative, nonradiative, and total decay rates of the excited state, respectively: α_b is the background absorption coefficient and α_r is the resonant absorption coefficient. Note that α_b does not contain the attenuation due to scattering, as this process does not lead to heating of the material. We have assumed that due to the small cross-section area of optical fibers, the fluorescence escape efficiency to be unity [3,19]. The mean fluorescence wavelength is defined by

$$\lambda_f(T) = \frac{\int_\Delta \lambda S(\lambda, T) d\lambda}{\int_\Delta S(\lambda, T) d\lambda}, \tag{4}$$

where $S(\lambda, T)$ is the fluorescence power spectral density, which is a function of the glass temperature T, and Δ is the spectral domain encompassing the relevant emission spectral range [16,18].

In order to achieve net solid-state optical refrigeration, it is necessary for the cooling efficiency to be positive. Therefore, we must show that $\eta_c > 0$ is attainable over a range of λ_p and T values. It can be seen from Eq. (1) that because λ_p and λ_f are often very close to each other in solid-state optical refrigeration schemes ($\lambda_p \gtrsim \lambda_f$), the internal quantum efficiency η_q has to be close to unity ($\eta_q \approx 1$) [3,16]. There are two main processes that lower the internal quantum efficiency: the multiphonon nonradiative relaxation and the concentration-quenching effect [20–27]. We will argue that the multiphonon nonradiative relaxation is negligible in Yb-doped silica glass and that the concentration-quenching process can be prevented if the Yb ion density is kept lower than the characteristic Yb ion-quenching concentration.

In order to evaluate the absorption efficiency η_{abs}, we need to know the background absorption (α_b) and resonant absorption (α_r) coefficients. For the background absorption coefficient in Yb-doped silica glass, we will use typical values reported in the literature [28–30]. By measuring the power spectral density of a Yb-doped silica optical fiber from its side at a range of temperatures, $S(\lambda, T)$, we can also obtain the resonant absorption coefficient (α_r) as well as the mean fluorescence wavelength (λ_f). Therefore, we will have all the necessary parameters in Eq. (1); using this information, we will estimate the cooling efficiency and show that solid-state optical refrigeration is feasible in Yb-doped silica glass.

II. THE INTERNAL QUANTUM EFFICIENCY

The internal quantum efficiency is the fraction of the radiative decay versus the total decay of an excited state in a medium; therefore, the presence of nonradiative decay channels characterized by the nonradiative decay rate W_{nr} in Eq. (2) is responsible for η_q decreasing below unity. The nonradiative decay channels in a typical Yb-doped silica glass can be broken down according to the following equation:

$$W_{\text{nr}} = W_{\text{mp}} + W_{\text{OH}}^{-} + W_{\text{Yb}} + \sum_{\text{TM}} W_{\text{TM}} + \sum_{\text{RE}} W_{\text{RE}}. \tag{5}$$

The partial nonradiative decay channels are as follows: W_{mp} represents the multiphonon decay of the Yb excited state, W_{OH}^{-} accounts for nonradiative decay of the Yb excited state via the high-energy vibrational modes of OH^- impurities, W_{Yb} accounts for nonradiative decay in Yb ion clusters, and W_{TM} and W_{RE} represent nonradiative decay due to interactions of the excited state with various transition-metal and rare-earth-ion impurities, respectively.

In the following, we will discuss the various nonradiative decay channels in Eq. (5) and show that they can be made sufficiently small to allow for a near-unity value of the internal quantum efficiency ($\eta_q \approx 1$). We begin with the multiphonon relaxation that originates from the coupling of the excited state with the vibrational wave functions of the ground state. Using the energy-gap law [20,22,24,31], we can calculate the decay rate from

$$W_{\text{mp}} = W_0 e^{-\alpha_h(E_g - 2E_p)}, \tag{6}$$

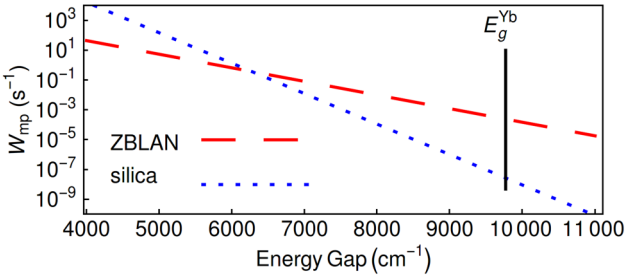

FIG. 1. The multiphonon nonradiative decay rate (W_{mp}) of Yb-doped ZBLAN and silica glasses versus the energy gap (E_g) calculated from Eq. (6) and the parameters listed in Table I.

where E_p is the maximum phonon energy of the host material and E_g is the energy gap of the dopant ion (Yb). W_0 and α_h are phenomenological parameters, the values of which depend strongly on the host material [20,22,24,31]. Figure 1 shows the multiphonon nonradiative decay rates of silica and ZBLAN glasses versus the energy gaps of the doped ions at $T = 300$ K, using the parameters shown in Table I.

The vertical solid line in Fig. 1 marks the energy gap of a Yb^{3+} ion. It is evident that for Yb-doped silica glass, the nonradiative decay rate is around $W_{mp}^{silica} \approx 10^{-8}$ s^{-1}, which is much smaller than the Yb-doped ZBLAN glass multiphonon decay rate $W_{mp}^{ZBLAN} \approx 10^{-4}$ s^{-1}. This comparison suggests that with respect to Yb multiphonon relaxation, silica glass is a more suitable choice for solid-state optical refrigeration than ZBLAN glass.

Considering the advances in materials synthesis of fiber preforms, the term W_{OH}^{-} in Eq. (5) can be made very small (see, e.g., dry-fiber technology [32]); therefore, it can be neglected [23]. It has also been shown by Auzel *et al.* [25] that the total effect of the last three terms in Eq. (5), $W_{Yb} + \Sigma W_{TM} + \Sigma W_{RE}$, can be described by a phenomenological equation based on a limited diffusion process, modeled as a nonradiative dipole-dipole interaction between the ions and impurities [25,26]. This concentration-quenching process can be prevented if the Yb ion density is lower than the critical quenching concentration of the Yb-doped silica glass, which exists because there are impurities. Therefore, the critical quenching concentration is generally a sample-specific quantity. That is, it would be higher for lower-impurity concentrations. For a Yb ion density smaller than the critical quenching concentration, the internal quantum efficiency can approach $\eta_q \approx 1$ [25–27]. It must be noted that an internal quantum efficiency of $\eta_q = 0.95$ is reported in [33] for Yb-doped silica, which is consistent with our claim that W_{nr} can be made quite small in Yb-doped silica.

TABLE I. Parameters related to Eq. (6) and Fig. 1 for silica and ZBLAN glasses [20,22,31].

Host	W_0 (s^{-1})	α_h (cm)	E_p (cm^{-1})
Silica	7.8×10^7	4.7×10^{-3}	1.10×10^3
ZBLAN	1.7×10^4	2.1×10^{-3}	0.58×10^3

III. ABSORPTION EFFICIENCY AND MEAN FLUORESCENCE WAVELENGTH

In order to calculate the cooling efficiency, we still need to obtain the resonant absorption coefficient and the mean fluorescence wavelength, both of which can be obtained from a spectroscopic investigation. The resonant absorption coefficient is used in conjunction with Eq. (3) to determine the absorption efficiency. The setup implemented in our experiment is shown in Fig. 2 and consists of a single-mode Yb-doped silica fiber (DF-1100, from Newport Corporation) that is pumped by a Ti:sapphire laser at $\lambda = 900$ nm. The fiber is mounted on a plate the temperature of which is varied from nearly 180 up to 360 K. The fluorescence of the Yb-doped silica fiber is captured by a multimode fiber from the side of the Yb-doped silica fiber and is sent to an optical spectrum analyzer (Yokogawa-AQ6319). Figure 3 shows the measured fluorescence spectra (power spectral density$S(\lambda, T)$),

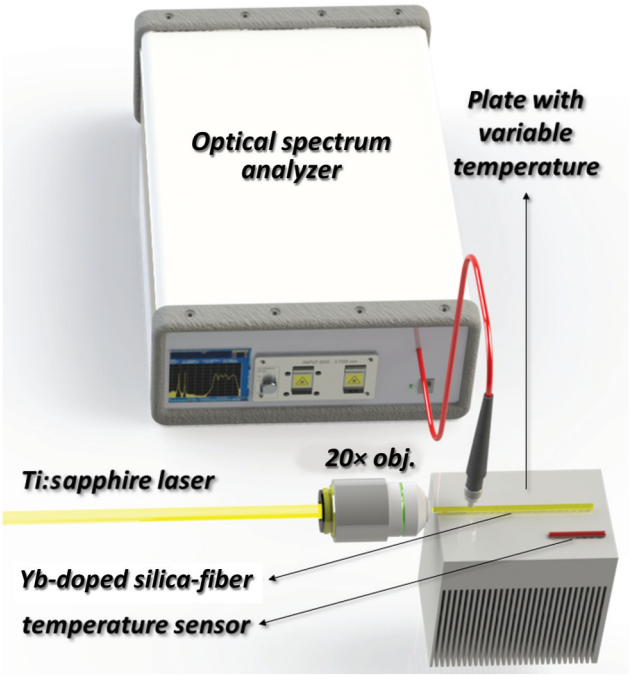

FIG. 2. The experimental setup is shown. A Ti:sapphire laser at $\lambda = 900$ nm is used to pump a single-mode Yb-doped silica fiber using a 20× objective lens. The fiber is mounted on a plate the temperature of which is varied from nearly 180 up to 360 K. The temperature of the plate is monitored by a temperature sensor. The fluorescence of the Yb-doped silica fiber is captured by a multimode fiber from the side of the Yb-doped silica fiber and is sent to an optical-spectrum analyzer.

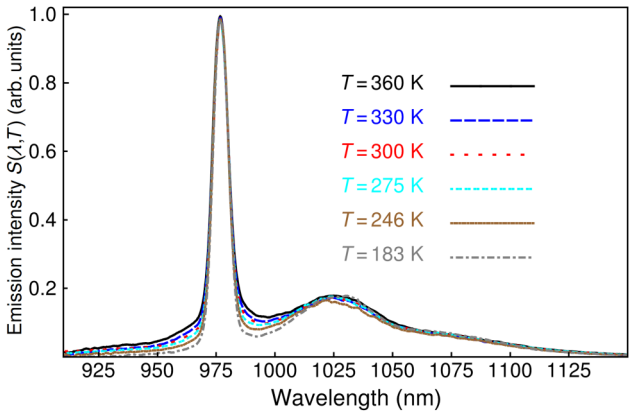

FIG. 3. Measured peak normalized emission spectra (fluorescence power spectral density) of DF-1100 Yb-doped silica fiber at a range of temperatures.

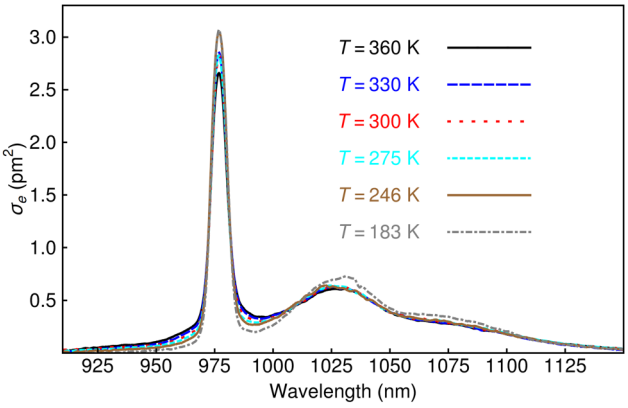

FIG. 4. The emission cross section versus the wavelength for DF-1000 Yb-doped silica fiber at a range of temperatures. The spectra are calculated from Eq. (8) using the emission spectra shown in Fig. 3 and the measured radiative lifetimes from Ref. [38].

normalized to their peak values at $\lambda_{\text{peak}} \approx 976$ nm, at a range of temperatures.

By inserting the measured fluorescence spectra into Eq. (4) and considering $\Delta \in \{905\text{nm}, 1150\text{nm}\}$, the dependence of the mean fluorescence wavelength on temperature is obtained. The mean fluorescence wavelength follows approximately the following formula:

$$\lambda_f(T) \approx 999(\text{nm}) + b \times T^{-1}, \quad b = 2735 \pm 31 \text{ nm/K}. \tag{7}$$

This behavior at temperatures within 245–360 K is nearly linear, which is similar to that reported in other host materials, such as ZBLAN [17,20].

In order to calculate the resonant absorption coefficient α_r, we first calculate the emission cross section σ_e and then use the McCumber relation to obtain the absorption cross section σ_a and then the resonant absorption coefficient α_r [34–36]. The emission cross section is obtained from the measured fluorescence power spectral density $S(\lambda, T)$ via the Füchtbauer-Ladenburg equation [36,37]:

$$\sigma_e(\lambda, T) = \frac{\lambda^5}{8\pi n^2 c \tau_r(T)} \times \frac{S(\lambda, T)}{\int_\Delta \lambda S(\lambda, T) d\lambda}, \tag{8}$$

where n is the refractive index of the fiber core, c is the speed of light in vacuum, and $\tau_r = W_r^{-1}$ is the radiative lifetime.

In order to apply Eq. (8), the radiative lifetime at each temperature needs to be measured. In high-quality samples, for which the nonradiative decay rates are negligible compared to the radiative decay rates, the fluorescence lifetimes are comparable to the radiative lifetimes ($\tau_f \approx \tau_r$); therefore, we measure the fluorescence lifetimes at various temperatures from the side of the fiber [38]. Using this assumption, the emission cross sections at various temperatures are calculated and are shown in Fig. 4. The absorption cross sections can be readily obtained using the McCumber relation:

$$\sigma_a(\lambda, T) = \sigma_e(\lambda, T) \times \mathcal{Z}(\lambda, T),$$
$$\mathcal{Z}(\lambda, T) = \exp\left[\frac{hc}{k_b T}\left(\frac{1}{\lambda} - \frac{1}{\lambda_0}\right)\right], \tag{9}$$

where k_b is the Boltzmann constant, h is the Planck constant, and $\lambda_0 = 976$ nm is the wavelength corresponding to the zero-line phonon energy [14,18,35]. The resonant absorption coefficient can be calculated from $\sigma_a(\lambda, T)$ in Eq. (9) (and Fig. 4) using

$$\alpha_r(\lambda, T) = \sigma_a(\lambda, T) \times N. \tag{10}$$

Here, we will assume a typical Yb ion density of $N = 5 \times 10^{25}$ m^{-3}. We now have all the necessary ingredients to calculate the cooling efficiency η_c in Eq. (1). We only need to provide a value for the background absorption coefficient in Eq. (3) to determine the absorption efficiency η_{abs}. Here, we assume a background absorption coefficient of $\alpha_b = 10$ dB/km $\approx 2.3 \times 10^{-3}$/m, which is a typical value for commercial-grade Yb-doped silica fibers. Using this information, we present a contour plot of the cooling efficiency η_c in Fig. 5 as a function of the pump wavelength and the temperature, assuming that $\eta_q = 1$. Note that we only know the values of $\alpha_r(\lambda, T)$ at discrete values of temperature T, for which our measurements are performed in Fig. 3; the density plot in Fig. 5 is an interpolation of the measured values. It can be seen in Fig. 5 that the cooling efficiency decreases with decreasing temperature; this behavior is due to the red-shift of the mean fluorescence wavelength and the decrease in the resonant absorption coefficient with decreasing temperature [16,20].

In practice, it is impossible to achieve an internal quantum efficiency of unity; therefore, in Fig. 6 we investigate

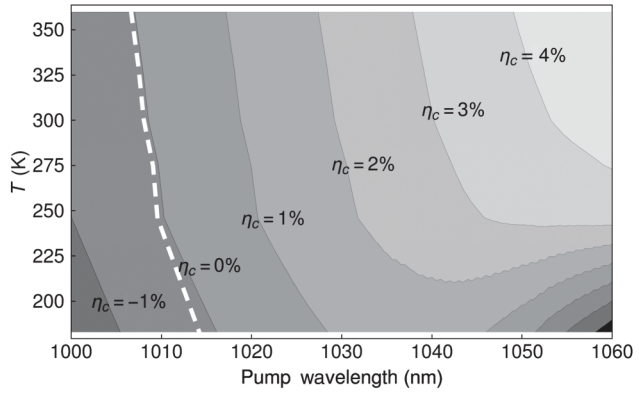

FIG. 5. The cooling efficiency versus the temperature and the pump wavelength with $\eta_q = 1$ and $\alpha_b = 10$ dB/km for DF-1100 Yb-doped silica fiber, calculated from Eq. (1). The dashed line connects the experimental measurements of the mean fluorescence wavelength versus the temperature.

the effect of a nonideal internal quantum efficiency on the cooling efficiency, for $\lambda_p = 1030$ nm, as a function of the temperature. The discrete points in Fig. 6 signify the values of η_c obtained for the assumed η_q at the particular measured temperatures reported in Fig. 3. The apparent difference between the cooling efficiency obtained for $\eta_q = 1$ versus $\eta_q = 0.98$ highlights the importance of having a high-quality glass for radiative cooling. While the discrete points in Fig. 6 reveal the main expected behavior of η_c versus the temperature, it is helpful to estimate the minimum achievable temperature for solid-state optical refrigeration in Yb-doped silica glass, subject to the assumptions made about η_q, N, and α_b. In order to do so, we next present an analytical fitting to the discrete points in Fig. 6 that can be used to estimate the minimum achievable temperature. The analytical fitting, which is described in the next paragraph, is used in conjunction with Eq. (1) to plot the colored lines for each value of η_q in Fig. 6 and is in reasonable agreement with the experimentally measured discrete data. From the discussions above and

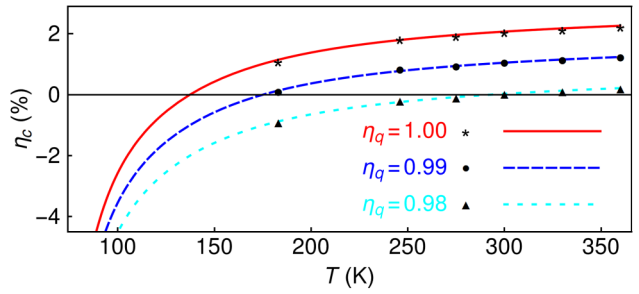

FIG. 6. The cooling efficiency versus the temperature with $\alpha_b = 10$ dB/km for DF-1100 Yb-doped silica fiber calculated from Eq. (1) for a range of internal quantum efficiencies, η_q. The colored lines are plotted using Eq. (1) and the fitting presented in Eq. (14).

Eqs. (8)–(10), we note that $\alpha_r(\lambda_p, T)$ (at the pump wavelength) can be expressed as follows:

$$\alpha_r(\lambda_p, T) \propto \frac{1}{c}\frac{\lambda_p^5}{\tau_r(T)} \times \frac{S(\lambda_p, T)}{\int_\Delta \lambda S(\lambda, T) d\lambda} \times \mathcal{Z}(\lambda_p, T). \quad (11)$$

In Ref. [38], we perform fluorescence-lifetime measurements in Yb-silica. Here, we present a fitting of $\tau_r(T)$ to an analytical form that is based on a two-level excited state:

$$\tau_r(T) = \frac{1 + \exp(-\delta E/k_b T)}{\tau_1^{-1} + \tau_2^{-1}\exp(-\delta E/k_b T)}, \quad (12)$$

in which $\tau_1 = 798 \pm 2$ μs and $\tau_2 = 576 \pm 27$ μs are the lifetimes of the first and second energy levels of the excited state, respectively, and $\delta E = 506 \pm 56$ cm^{-1} is the energy difference between these two levels [36,39]. We also present the following approximation:

$$\frac{\lambda_p^2 S(\lambda_p, T)}{\int_\Delta \lambda S(\lambda, T) d\lambda} \approx 7.4 + \left(\frac{d}{T}\right)^5, \quad d = 205.9 \pm 2.4 \text{ K}. \quad (13)$$

Using Eqs. (12) and (13), we can approximate $\alpha_r(\lambda_p, T)$ [Eq. (11)] with the following mathematical form:

$$\alpha_r(\lambda_p, T) \approx \frac{\alpha_{r,0}}{c\tau_r(T)} \times (7.4 + (d/T)^5) \times \mathcal{Z}(\lambda_p, T). \quad (14)$$

By fitting the analytical in Eq. (14) to the discrete points in Fig. 6, we find the dimensionless coefficient $\alpha_{r,0} = (0.95 \pm 0.01) \times 10^6$. The fitted lines in Fig. 6 show that the minimum achievable temperature can reach down to $T_{\min} = 138$ K for $\eta_q = 1$, $T_{\min} = 175$ K for $\eta_q = 0.99$, and $T_{\min} = 290$ K for $\eta_q = 0.98$. Figure 6 also shows that the maximum cooling efficiency for Yb-silica glass is around $\eta_c^{\max} \approx 2\%$ at room temperature for $\lambda_p = 1030$ nm. Setting the background absorption to zero ($\alpha_b = 0$) increases this value to $\eta_c^{\max} \approx 2.2\%$. In order to increase the cooling efficiency, the background absorption must be minimized, the internal quantum efficiency has to be close to unity, and the ion-dopant density N must be increased to enhance the resonant absorption coefficient. We note that these requirements are not necessarily compatible with each other; e.g., increasing N can potentially decrease η_q due to quenching. Therefore, a compromise determined by careful measurements must be obtained.

IV. DISCUSSION AND CONCLUSION

It must be noted that by taking $N = 5 \times 10^{25}$ m^{-3} in this paper, we have implicitly assumed that the silica glass host is codoped with some modifiers such as Al_2O_3, in order to shift the quenching concentration to higher values to reduce clustering and ensure an adequate cooling efficiency [40,41]. For pure silica, applying the

model developed by Auzel *et al.* [25] to the experimental data from Ref. [23], it can be shown that $N = 0.7 \times 10^{25}$ m^{-3} can guarantee a near-unity internal quantum efficiency [40,41]. Using $N = 0.7 \times 10^{25}$ m^{-3} in pure silica, we calculate the minimum achievable temperature to be $T_{\min} = 216$ K for $\eta_q = 1$, and $T_{\min} = 262$ K for $\eta_q = 0.99$. For $\eta_q = 0.98$, $T_{\min}$ is above room temperature. As expected, a decrease in ion density results in a lower cooling efficiency.

In conclusion, we argue that a high-purity Yb-doped silica glass can potentially be cooled via anti-Stokes fluorescence. In order to achieve net solid-state optical refrigeration, it is necessary for the cooling efficiency to be positive. This requires the pump wavelength to be greater than the mean fluorescence wavelength and the internal quantum efficiency as well as the absorption efficiency to be near unity. For the internal quantum efficiency we show that, in principle, the nonradiative decay rate $W_{\rm nr}$ can be made substantially smaller than the radiative decay rate W_r. Therefore, an internal quantum efficiency of near unity can be obtained, making Yb-doped silica glass suitable for solid-state optical refrigeration. Our assessment is based on reasonable assumptions for material properties, e.g., we assume a typical background absorption coefficient of $\alpha_b = 10$ dB/km and an internal quantum efficiency of larger than $\eta_q = 0.98$. We perform spectral measurements of the fluorescence from a Yb-doped silica optical fiber at a range of temperatures. Using these measurements, we report the temperature dependence of the mean fluorescence wavelength and estimate the minimum achievable temperature in Yb-doped silica glass.

Our analysis highlights the potential for Yb-doped silica glass to be used as the gain medium for radiation-balanced high-power fiber lasers and amplifiers. In order to observe the solid-state optical refrigeration of silica, high-quality samples with adequate Yb doping concentrations are required. It is preferable to codope silica with modifiers such as Al_2O_3 to increase the solubility of Yb ions and consequently increase the cooling efficiency. Of course, proper thermal isolation in solid-state optical refrigeration is essential. Such experiments are quite delicate [16] and Yb-doped silica will be no exception.

ACKNOWLEDGMENTS

This material is based upon work supported by the Air Force Office of Scientific Research under Award No. FA9550-16-1-0362, entitled Multidisciplinary Approaches to Radiation Balanced Lasers (MARBLE).

[1] P. Pringsheim, Zwei Bemerkungen über den Unterschied von Lumineszenz- und Temperaturstrahlung, Z. Phys. **57**, 739 (1929).

[2] L. Landau, On the thermodynamics of photoluminescence, J. Phys. **10**, (1946).

[3] R. I. Epstein, M. I. Buchwald, B. C. Edwards, T. R. Gosnell, and C. E. Mungan, Observation of laser-induced fluorescent cooling of a solid, Nature **377**, 500 (1995).

[4] R. I. Epstein, and M. Sheik-Bahae, *Optical Refrigeration: Science and Applications of Laser Cooling of Solids* (John Wiley & Sons, Weinheim, Germany, 2010).

[5] D. V. Seletskiy, R. Epstein, and M. Sheik-Bahae, Laser cooling in solids: Advances and prospects, Rep. Prog. Phys. **79**, 096401 (2016).

[6] D. J. Richardson, J. Nilsson, and W. A. Clarkson, High power fiber lasers: Current status and future perspectives, J. Opt. Soc. Am. B **27**, B63 (2010).

[7] A. V. Smith, and J. J. Smith, Mode instability in high power fiber amplifiers, Opt. Express **19**, 10180 (2011).

[8] J. W. Dawson, M. J. Messerly, R. J. Beach, M. Y. Shverdin, E. A. Stappaerts, A. K. Sridharan, P. H. Pax, J. E. Heebner, C. W. Siders, and C. Barty, Analysis of the scalability of diffraction-limited fiber lasers and amplifiers to high average power, Opt. Express **16**, 13240 (2008).

[9] C. Jauregui, T. Eidam, H.-J. Otto, F. Stutzki, F. Jansen, J. Limpert, and A. Tünnermann, Physical origin of mode instabilities in high-power fiber laser systems, Opt. Express **20**, 12912 (2012).

[10] S. R. Bowman, Lasers without internal heat generation, IEEE J. Quantum Electron. **35**, 115 (1999).

[11] S. R. Bowman, S. P. O'Connor, S. Biswal, N. J. Condon, and A. Rosenberg, Minimizing heat generation in solid-state lasers, IEEE J. Quantum Electron. **46**, 1076 (2010).

[12] E. Mobini, M. Peysokhan, B. Abaie, and A. Mafi, Thermal modeling, heat mitigation, and radiative cooling for double-clad fiber amplifiers, J. Opt. Soc. Am. B, **35**, 2484 (2018).

[13] G. Nemova, and R. Kashyap, Athermal continuous-wave fiber amplifier, Opt. Commun. **282**, 2571 (2009).

[14] H. Pask, R. J. Carman, D. C. Hanna, A. C. Tropper, C. J. Mackechnie, P. R. Barber, and J. M. Dawes, Ytterbium-doped silica fiber lasers: Versatile sources for the 1-1.2 μm region, IEEE J. Sel. Top. Quantum Electron. **1**, 2 (1995).

[15] R. Paschotta, J. Nilsson, A. C. Tropper, and D. C. Hanna, Ytterbium-doped fiber amplifiers, IEEE J. Quantum Electron. **33**, 1049 (1997).

[16] D. V. Seletskiy, S. D. Melgaard, S. Bigotta, A. Di Lieto, M. Tonelli, and M. Sheik-Bahae, Laser cooling of solids to cryogenic temperatures, Nat. Photonics **4**, 161 (2010).

[17] G. Lei, J. E. Anderson, M. I. Buchwald, B. C. Edwards, R. I. Epstein, M. T. Murtagh, and G. Sigel, Spectroscopic evaluation of Yb^{3+}-doped glasses for optical refrigeration, IEEE J. Quantum Electron. **34**, 1839 (1998).

[18] S. Melgaard, D. Seletskiy, M. Sheik-Bahae, S. Bigotta, A. Di Lieto, M. Tonelli, and R. Epstein, in *Laser Refrigeration of Solids III* (International Society for Optics and Photonics, 2010), Vol. 7614, p. 761407.

[19] X. Ruan, and M. Kaviany, Enhanced laser cooling of rare-earth-ion-doped nanocrystalline powders, Phys. Rev. B **73**, 155422 (2006).

[20] M. P. Hehlen, R. I. Epstein, and H. Inoue, Model of laser cooling in the Yb^{3+}-doped fluorozirconate glass ZBLAN, Phys. Rev. B **75**, 144302 (2007).

[21] M. J. Digonnet, *Rare-Earth-Doped Fiber Lasers and Amplifiers, Revised and Expanded* (CRC Press, New York, NY, 2001).

[22] C. Hoyt, M. Hasselbeck, M. Sheik-Bahae, R. Epstein, S. Greenfield, J. Thiede, J. Distel, and J. Valencia, Advances in laser cooling of thulium-doped glass, J. Opt. Soc. Am. B, **20**, 1066 (2003).

[23] P. Barua, E. Sekiya, K. Saito, and A. Ikushima, Influences of Yb^{3+} ion concentration on the spectroscopic properties of silica glass, J. Non-Cryst. Solids **354**, 4760 (2008).

[24] J. Van Dijk, and M. Schuurmans, On the nonradiative and radiative decay rates and a modified exponential energy gap law for $4f$ -$4f'$ transitions in rare-earth ions, J. Chem. Phys. **78**, 5317 (1983).

[25] F. Auzel, G. Baldacchini, L. Laversenne, and G. Boulon, Radiation trapping and self-quenching analysis in Yb^{3+}, Er^{3+}, and Ho^{3+} doped Y_2O_3, Opt. Mater. **24**, 103 (2003).

[26] G. Boulon, Why so deep research on Yb^{3+}-doped optical inorganic materials? J. Alloys Compd. **451**, 1 (2008).

[27] D. T. Nguyen, J. Zong, D. Rhonehouse, A. Miller, Z. Yao, G. Hardesty, N. Kwong, R. Binder, and A. Chavez-Pirson, in *Laser Refrigeration of Solids V* (International Society for Optics and Photonics, San Francisco, California, USA, 2012), Vol. 8275, p. 827506.

[28] S. Jetschke, S. Unger, A. Schwuchow, M. Leich, and J. Kirchhof, Efficient Yb laser fibers with low photodarkening by optimization of the core composition, Opt. Express **16**, 15540 (2008).

[29] M. Leich, F. Just, A. Langner, M. Such, G. Schötz, T. Eschrich, and S. Grimm, Highly efficient Yb-doped silica fibers prepared by powder sinter technology, Opt. lett. **36**, 1557 (2011).

[30] R. Sidharthan, S. H. Lim, K. J. Lim, D. Ho, C. H. Tse, J. Ji, H. Li, Y. M. Seng, S. L. Chua, and S. Yoo, in *Conference on Lasers and Electro-Optics* (Optical Society of America, San Jose, California, USA, 2018), p. JTh2A.129.

[31] B. Faure, W. Blanc, B. Dussardier, and G. Monnom, Improvement of the Tm^{3+}: $^3H_4$ level lifetime in silica optical fibers by lowering the local phonon energy, J. Non-Cryst. Solids **353**, 2767 (2007).

[32] G. A. Thomas, B. I. Shraiman, P. F. Glodis, and M. J. Stephen, Towards the clarity limit in optical fibre, Nature **404**, 262 (2000).

[33] Y. Jeong, J. K. Sahu, D. N. Payne, and J. Nilsson, Ytterbium-doped large-core fiber laser with 1.36 kW continuous-wave output power, Opt. Express **12**, 6088 (2004).

[34] T. Fan, and M. Kokta, End-pumped $Nd:LaF^{3+}$ and $Nd:LaMgAl_{11}O_{19}$ lasers, IEEE J. Quantum Electron. **25**, 1845 (1989).

[35] D. E. McCumber, Theory of phonon-terminated optical masers, Phys. Rev. **134**, A299 (1964).

[36] T. Newell, P. Peterson, A. Gavrielides, and M. Sharma, Temperature effects on the emission properties of Yb-doped optical fibers, Opt. Commun. **273**, 256 (2007).

[37] B. Aull, and H. Jenssen, Vibronic interactions in Nd:YAG resulting in nonreciprocity of absorption and stimulated emission cross sections, IEEE J. Quantum Electron. **18**, 925 (1982).

[38] E. Mobini, M. Peysokhan, B. Abaie, and A. Mafi, in *Conference on Lasers and Electro-Optics* (Optical Society of America, San Jose, California, USA, 2018), p. FF3E.4.

[39] Z. Zhang, K. Grattan, and A. Palmer, Thermal characteristics of alexandrite fluorescence decay at high temperatures, induced by a visible laser diode emission, J. Appl. Phys. **73**, 3493 (1993).

[40] K. Arai, H. Namikawa, K. Kumata, T. Honda, Y. Ishii, and T. Handa, Aluminum or phosphorus co-doping effects on the fluorescence and structural properties of neodymium-doped silica glass, J. Appl. Phys. **59**, 3430 (1986).

[41] J. Lægsgaard, Dissolution of rare-earth clusters in SiO_2 by Al codoping: A microscopic model, Phys. Rev. B **65**, 174114 (2002).